Clinical Radiology 74 (2019) 187–195

Contents lists available at ScienceDirect

Clinical Radiology

journal homepage: www.clinicalradiologyonline.net

Comparison of the ^{18}F-FDG avidity at PET of benign and malignant pure ground-glass opacities: a paradox?

S. McDermott [a], A. Kilcoyne [b], Y. Wang [c], J.A. Scott [c], E.F. Halpern [d], J.B. Ackman [a,*]

[a] *Division of Thoracic Imaging and Intervention, MGH Department of Radiology, Founders House 202, 55 Fruit Street, Boston, MA 02114, USA*
[b] *Division of Abdominal Imaging, MGH Department of Radiology, 55 Fruit Street, Boston, MA 02114, USA*
[c] *Division of Nuclear Medicine and Molecular Imaging, MGH Department of Radiology, 55 Fruit Street, Boston, MA 02114, USA*
[d] *MGH Institute for Technology Assessment, 101 Merrimac St, Boston, MA 02114, USA*

ARTICLE INFORMATION

Article history:
Received 15 August 2018
Accepted 13 December 2018

AIM: To determine if pure ground-glass opacities (GGOs) and the subgroup of ground-glass nodules (GGNs) typically demonstrate higher 2-[^{18}F]-fluoro-2-deoxy-D-glucose (^{18}F-FDG) uptake at positron-emission tomography (PET) when benign than when malignant.

MATERIALS AND METHODS: Informed consent was waived for this institutional review board (IRB)-approved, Health Insurance Portability and Accountability Act (HIPAA) compliant, retrospective study. A review of all 1,864 combined PET/computed tomography (CT) examinations performed in 2011 on a single system to identify pure GGOs with mean diameter ≥1 cm yielded 166 GGOs. Two blinded subspecialty-trained thoracic radiologists independently assessed GGO size, morphology, attenuation, and location on CT. A blinded nuclear radiologist procured the SUVmax for each GGO. Final diagnosis of malignancy (n=21) was made based on histopathology or upon increased size and attenuation; a final diagnosis of benignity (n=106) was made if GGO resolved, was new within 3 months, evolved in a manner consistent with pulmonary fibrosis, or was stable for ≥60 months; 29 were indeterminate and were excluded, along with 10 cases with unreliable SUVmax measurements, yielding 127 GGOs, of which 68 were GGNs, in 76 patients.

RESULTS: The SUVmax was significantly higher in benign than malignant GGOs (p=0.0017) and in the GGN subgroup (p=0.03). A threshold SUVmax >1.5 for GGOs, including GGNs, assured benignity in this cohort.

CONCLUSION: Benign GGOs and the benign GGN subgroup demonstrated significantly higher FDG uptake at PET than malignant GGOs/GGNs. Awareness of this finding may prevent misinterpretation of highly ^{18}FDG-avid pure GGOs/GGNs as definitively malignant, which could lead to unnecessary thoracic surgery and its associated risks.

* Guarantor and correspondent: J. B. Ackman, MGH Department of Radiology, Division of Thoracic Imaging and Intervention, Founders House 202, 55 Fruit Street, Boston, MA 02114, USA. Tel.: +1(617) 724 4254; fax: +1(617) 724 0046.
E-mail address: jackman@mgh.harvard.edu (J.B. Ackman).

https://doi.org/10.1016/j.crad.2018.12.009
0009-9260/

Introduction

Over the past decade, healthcare providers have increasingly relied on combined 2-[^{18}F]-fluoro-2-deoxy-D-glucose (^{18}FDG) positron-emission tomography/computed tomography (PET/CT) imaging to distinguish benign from malignant pulmonary nodules on account of expected higher rates of glucose metabolism in malignant lesions; however, the ability to make this distinction at ^{18}FDG-PET/CT has been shown to vary with nodule constitution, whether solid or subsolid.

Lung adenocarcinoma subtypes, which can manifest as pure ground-glass opacities (GGOs) include adenocarcinoma in-situ, minimally invasive adenocarcinoma, and rarely, invasive adenocarcinoma.[1] Possible causes for low glucose metabolism and thereby false-negative ^{18}F-FDG-PET results in these tumours include low cellularity, low degree of nuclear atypia, desmoplasia, high proportion of mucin content, necrosis, and a low density of viable cancer cells.[2–5] In contradistinction, inflammatory GGOs can yield false-positive ^{18}F-FDG-PET results.[2,6,7]

Early studies suggested a maximum standard uptake value (SUVmax) threshold of 2.5 as a sensitive and specific means for differentiating benign from malignant pulmonary nodules.[8–11] Although this threshold is a somewhat helpful guide for solid nodules, it is less helpful for subsolid nodules. In fact, indolent lung malignancies, which may have subsolid components on CT, can result in false-negative ^{18}F-FDG-PET results.[3,12–14] Unfortunately, prior studies examining the usefulness of ^{18}F-FDG-PET for distinguishing malignant from benign pulmonary nodules have not always differentiated between solid, part-solid, and pure ground-glass nodules (GGNs),[15–18]

More recent studies have shown greater ^{18}FDG avidity for benign than malignant subsolid nodules, but either merged both pure GGNs and part-solid nodules in their analysis and/or used histograms to define and identify them,[19–21] rather than applying the widely accepted Fleischner Society definition of GGNs.[22] The latter requires qualitative visual inspection, rather than quantitative analysis, and is therefore of more practical clinical use and has been used in daily clinical practice for decades. Use of histograms to identify GGOs is not standard clinical practice. In addition, a review of the figures within the article upon which histogram analysis in the above cited papers was based[23] reveals that histogram use yielded inclusion of part-solid nodules in their ground-glass cohort, confounding their results and rendering them potentially inapplicable to pure GGOs.

The Fleischner Society glossary of terms defines a GGO on CT as an area of increased pulmonary parenchymal attenuation that does not obscure bronchovascular structures. It defines a nodule as a rounded opacity $\leq$3 cm. A GGN possesses both of these qualifications.[22] Although the causes of GGOs are numerous and include pulmonary oedema, haemorrhage, infection, inflammation, and interstitial lung disease, they also include atypical adenomatous hyperplasia, a premalignant lesion, and indolent lung cancer.[24] Therefore, persistent GGOs often require at least 5 years of surveillance.[25]

Based on expectations related to differences in metabolism and observational experience with ^{18}FDG-PET/CT, it was hypothesised that, counter to prevalent expectation, benign pure GGOs and the benign pure GGN subgroup, as defined by Fleischner criteria, are apt to exhibit greater ^{18}FDG avidity at PET than malignant pure GGOs/GGNs. If borne out to be true, the importance of this knowledge would be to prevent misinterpretation of highly ^{18}FDG-avid pure GGOs/GGNs as malignant, which could lead to unnecessary diagnostic intervention and its associated risks.

The purpose of this study was to determine if pure GGOs (nodular and non-nodular) and the GGN subgroup typically demonstrate higher ^{18}FDG uptake when benign than when malignant.

Materials and methods

Approval for this Health Insurance Portability and Accountability Act (HIPAA)-compliant, retrospective study was obtained from the institutional review board. The requirement for informed consent was waived.

Scan selection

A list of all PET/CT examinations with a concurrent diagnostic chest CT with intravenous contrast medium, performed for any indication on a single PET/CT system (Siemens Biograph 64; Erlangen, Germany) at a quaternary referral hospital from 1 January to 31 December 2011 was obtained. A random number generator randomised the order of these scans. All studies were subsequently reviewed in this prescribed random order to identify solely focal, measureable, pure GGOs, whether nodular (GGNs) or non-nodular, with a mean diameter $\geq$10 mm, exclusively on the 1.5 mm slice series. Part-solid lesions were excluded. If a patient underwent more than one PET/CT examination over the 12 months, the first scan on the randomised list of a given patient was the scan included in this study. Scans were excluded if there were no GGOs or diffuse GGOs, if no thin 1.5 mm collimation series was available, or if images were degraded by respiratory motion. Paediatric patients ($\leq$18 years of age) were also excluded.

Integrated FDG-PET/CT acquisition

Each integrated FDG PET/CT study included a low-dose non-diagnostic CT examination for attenuation correction purposes only, an ^{18}F-FDG-PET examination, and a diagnostic CT examination with iodinated contrast medium, all of which were performed on the same system during the same imaging appointment. Separate low-dose attenuation correction and diagnostic CT examinations were performed to avoid errors in attenuation correction related to the presence of intravenous and oral contrast media.

The non-diagnostic attenuation correction, low-dose, unenhanced CT examination was performed using 120

kVp, modulated tube current dependent on body mass index (BMI; 11 mA for BMI <30, 30 mA for BMI of 30–34, 40 mA for BMI of 35–44, and 100 mA for BMI >45), a tube rotation time of 0.5 seconds per rotation, a pitch of 1.5, and a section thickness of 5 mm.

A PET examination was obtained over the same anatomical regions promptly after the non-diagnostic CT in seven table positions, at 3 minutes per bed position for patients with BMI <30, 4 minutes per bed position for BMI of 30–34, 5 minutes per bed position for BMI of 35–44, and 6 minutes per bed position for BMI >45. Iterative reconstruction of the PET data was performed with segmented correction for attenuation using the low-dose CT data, with a final section thickness of 5 mm. Each patient fasted at least 6 hours prior to FDG administration. A blood glucose level was procured just before FDG injection to exclude hyperglycaemic patients. The mean glucose level of the present study cohort was 110±15 mg/dl (range 86–138 mg/dl). A single intravenous injection of 15.8±2.2 mCi (584±81 MBq) of FDG was therefore administered, as per national standards for blood glucose levels ≤250 mg/dl. The patients were scanned approximately 1 hour after injection by an integrated 64-slice PET/CT system. They were instructed to breathe shallowly during the PET examination.

Following the PET acquisition, a diagnostic CT examination with iodinated intravenous contrast medium was obtained using the following parameters: 120kVp, modulated tube current, a tube rotation time of 0.5 seconds per rotation, a variable pitch between 1–1.5, depending on patient BMI, and a section thickness of 2 mm. Coronal and sagittal reformats in 2 mm slice thickness and axial super dimension reformats in 1.5 mm slice thickness were also reconstructed. Patients were instructed to hold their breath at mid-inspiration for this diagnostic CT examination.

CT image analysis

Two fellowship-trained thoracic radiologists, with 21 and 7 years of experience, blinded to patient history and final diagnosis of the GGO, independently assessed the CT examinations. The thin-section CT (1.5 mm) images were reviewed and analysed on a picture archiving and communication system (PACS) workstation (AGFA IMPAX 6.6.1.3004) that allowed the readers to measure the long and short axis of the GGOs and to draw regions-of-interest (ROI) to obtain attenuation values measurements. All images were displayed at lung window settings (centre −550 HU, width 1,500 HU).

A maximum of five focal, measureable, GGOs ≥10 mm in mean diameter, were identified and analysed per scan. Long and short axis measurements and mean attenuation values with standard deviation of each GGO were obtained and recorded independently by each reader, with results averaged prior to statistical analysis. The mean and standard deviation of the attenuation of the GGO was obtained by placing a round or elliptical ROI encompassing the largest area of the opacity and excluding vessels to the extent possible. Provided the GGO was focal and measureable, it was included in the study, whether it met the Fleischner Society definition of a nodule and was both of ground-glass attenuation and ≤3 cm (GGN) or it was a non-nodular (non-rounded), focal measurable GGO. GGOs were then classified morphologically as nodular GGOs (GGNs) and non-nodular GGOs (Fig 1). Any disagreement regarding morphology was resolved by consensus.

PET image analysis

PET image analysis was performed on dedicated multimodality viewing software (Siemens SyngoVia VB20; Erlangen, Germany) by a single nuclear radiologist with 4 years of experience. Each GGO, identified on thin 1.5 mm

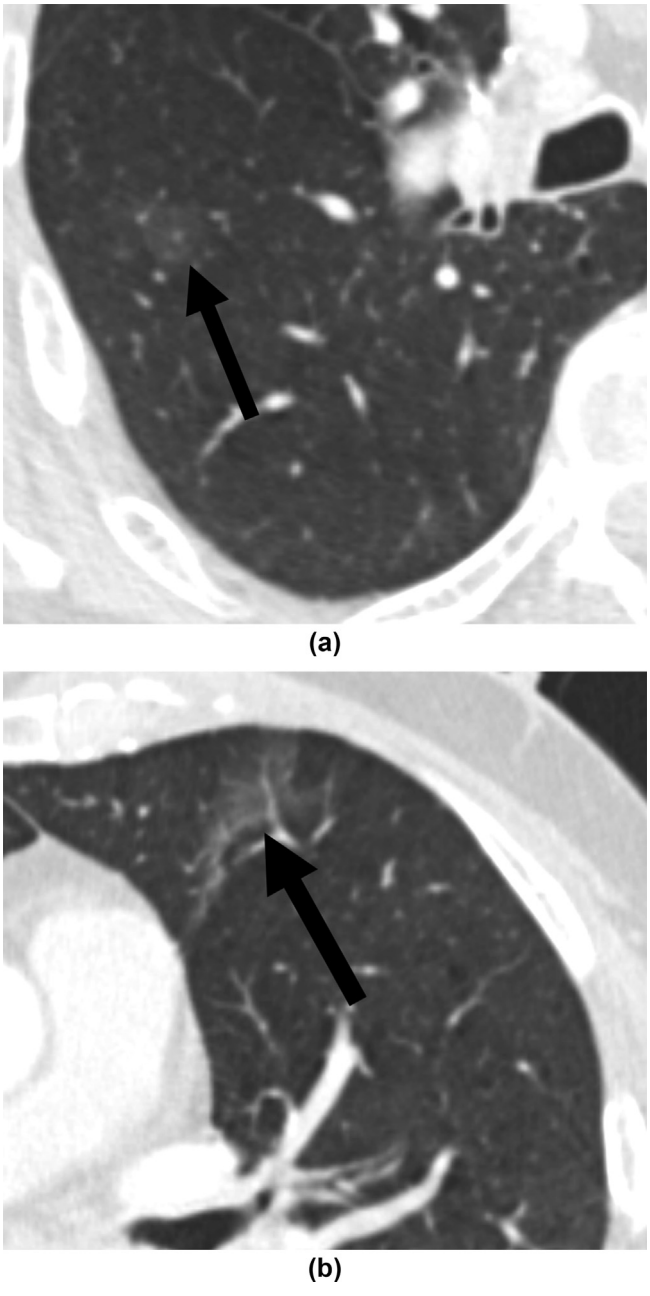

Figure 1 Morphologic classification. Axial CT images demonstrating (a) a nodular GGO (GGN; arrow) and (b) a non-nodular GGO (arrow).

slice, super-dimension reformat CT imaging, was localised manually on the low-dose non-diagnostic CT scan performed for attenuation correction purposes. An ROI, inclusive of the entire opacity, was drawn on the low-dose CT image and automatically mapped to the co-registered PET image to measure SUVmax. Visual analysis was performed to confirm that the ROI on the PET image was appropriate. If the opacity was in an area where SUV measurements cannot be reliably measured, for example, near the diaphragm, the GGO was excluded. A reference ROI measuring 3 cm^2 was drawn in the right hepatic lobe in a region without evident anatomical abnormalities by CT, and the mean SUV was acquired, hereby referred to as SUV_{liver}. The corrected SUVmax ($SUVmax_{corr}$) was calculated for each GGO by dividing SUVmax by SUV_{liver}.

Final diagnosis

The final diagnosis was made based on histopathology, if available. When histopathology was unavailable, determination of malignancy versus benignity was made by assessment of GGO behaviour over time on prior and follow-up imaging, as per standard clinical practice. A GGO was considered malignant if malignant cells were identified at biopsy or surgery or if the GGO increased in size and attenuation over an interval greater than 6 months (example in Fig 2). A GGO was considered benign if the opacity resolved, decreased in size and attenuation over 3 months or a longer period in the absence of chemotherapy, had arisen ($\geq$1cm) within 3 months, was stable for >5 years,[25] or had imaging features that evolved in a manner consistent with interstitial lung disease or radiation fibrosis[26,27] in patients with appropriate clinical history (Fig 3). If a benign or malignant determination could not be made, the lesion was considered indeterminate.

Statistical analysis

Statistical analysis was performed with SAS (version 9.4; SAS Institute, Cary, NC, USA) by two-sided Wilcoxon rank sum test and Fisher's exact test, as appropriate. A p-value of <0.05 was considered statistically significant.

Results

In 2011, a total of 1,864 PET/CT examinations were performed on 1,418 patients on the single PET/CT system utilised for this investigation. Exclusion of duplicate patients left 1,418 PET/CT examinations. After image review and application of the inclusion and exclusion criteria, 108 scans remained with 166 GGOs. Ten GGOs were subsequently excluded because an accurate SUV measurement could not be obtained on account of proximity to FDG-avid structures. An additional 29 GGOs were excluded, as a final diagnosis of benignity or malignancy could not be established (indeterminate), based on the standard, widely accepted and used clinical criteria described in the Final Diagnosis section of the Materials and Methods. That is, a minority of GGOs did not fall into any of the clinically diagnostic categories and therefore could not be categorised as benign or malignant. The final study cohort consisted of 127 nodular and non-nodular GGOs in 76 patients. Amidst these 127 GGOs were 68 GGNs, of which 48 were benign and 20 malignant, and 59 non-nodular GGOs, of which 58 were benign and one malignant (Fig 4 provides a flowchart of the subject enrolment process).

The present cohort consisted of 37 men and 39 women with an average age of 62 years (range 20–91 years). Forty-nine (23 men, 26 women) were current or former smokers. The indications for the PET/CT examinations in which the 127 GGOs were encountered are listed in Table 1. Each

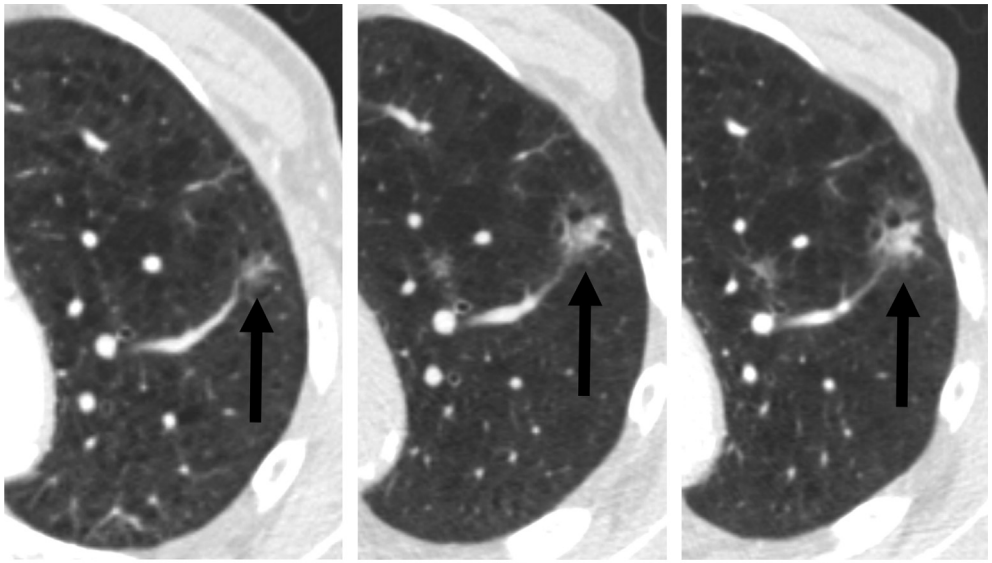

Figure 2 Final diagnosis determination: malignant. An 85-year-old man with a history of lung cancer and (a) a 12 mm mean diameter GGN on axial CT (arrow). This GGN increased in size and attenuation on follow-up imaging performed (b) 6 months and (c) 9 months later.

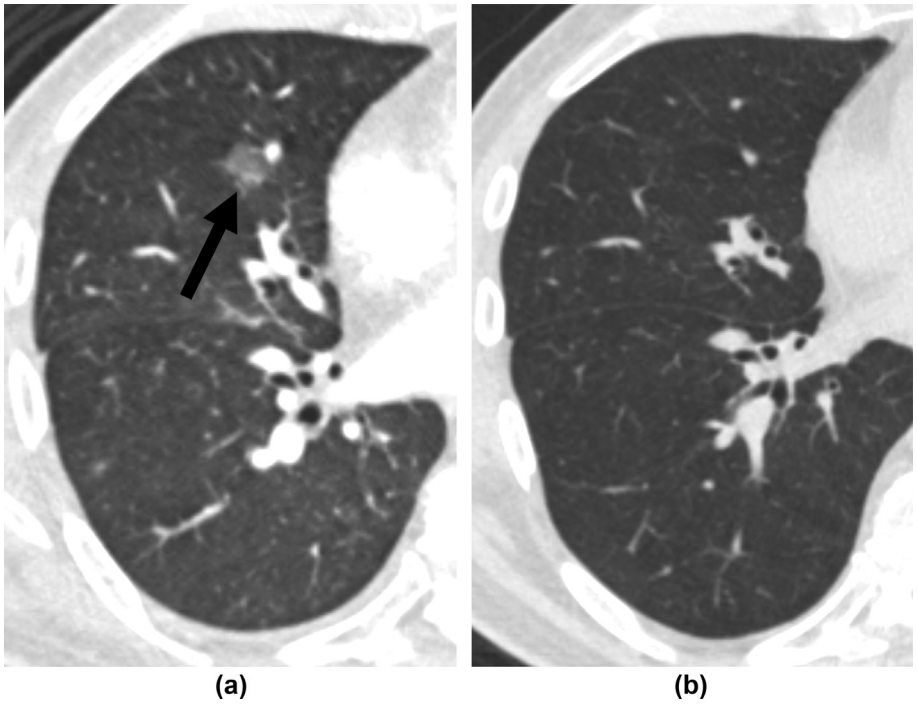

Figure 3 Final diagnosis determination: benign. A 42-year-old man with lymphoma and (a) an 11 mm mean diameter GGN on axial CT (arrow), which resolved on a subsequent chest CT performed 3 months later (b), in the absence of therapy for lymphoma.

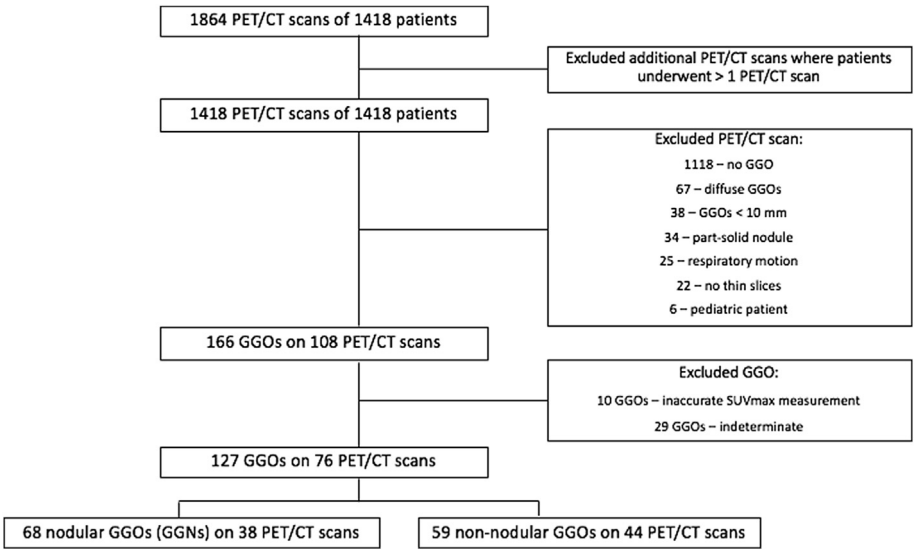

Figure 4 Flowchart of study population selection from all patients who underwent FDG-PET/CT imaging on a single PET/CT system in 2011.

patient had an average of 1.7 GGO, ranging from one to a limit of five GGOs (51 patients had a single GGO, 11 had two, five had three, six had four, and three had five). Table 2 provides the criteria used to determine benignity versus malignancy of the GGOs included in this study and the number and percentage of GGOs meeting each of these criteria.

Table 3 shows how the demographic findings of sex, age, smoking history, history of lung cancer, and history of extrapulmonary malignancy related to benign or malignant final diagnosis.

Regarding CT imaging features, benign GGOs were significantly larger than malignant GGOs (mean diameter of 25 mm, with range of 10–78 mm versus a mean diameter of 14 mm, with range of 10–26 mm, respectively, $p<0.0001$). Subgroup analysis of GGNs (excluding non-nodular GGOs) revealed benign GGNs to be larger than malignant GGNs (mean diameter of 18 mm, median diameter of 15 mm, and range of 10–42 mm versus mean diameter of 14 mm, median diameter of 12 mm, and range of 10–26 mm; $p=0.01$). There was a significant difference regarding the location of the GGOs, with 62% (13/21) of malignant GGOs occurring in

Table 1
Indications[a] for combined 2-[^{18}F]-fluoro-2-deoxy-D-glucose (^{18}FDG) positron-emission tomography/computed tomography (PET/CT) in the study cohort (n=127 GGOs).

Indication for PET/CT per GGO/GGN, as provided in the radiology information system (RIS)	No. of cases with indication
Abnormal chest CT	2
Breast cancer	3
Cervical cancer	2
Colon cancer	5
Endometrial cancer	1
Oesophageal cancer	9
Gastroesophageal junction cancer	2
Head and neck cancer (non-thyroid)	5
Idiopathic thrombocytopenic purpura	1
Lung cancer	39
Lung mass	3
Lymphoma (non-Hodgkin)	25
Lymphoma (Hodgkin)	6
Melanoma	8
Myasthenia, diffuse mediastinal lymphadenopathy	1
Neuroendocrine tumour	1
Ovarian cancer	1
Pancreatic cancer	1
Prostate and thyroid cancer	1
Pulmonary nodule	1
Pulmonary nodules, mediastinal lymphadenopathy	4
Scalp cancer	2
Soft-tissue sarcoma	2
Unknown primary	2

GGOs, ground-glass opacities; GGNs, ground-glass nodules.
[a] As originally provided by healthcare provider in radiology order entry system.

the upper lobes compared to 57% (60/106) of benign GGOs occurring in the upper lobes (p=0.0088). There was a significant difference in morphology between malignant and benign GGOs, with 95% (20/21) of malignant GGOs exhibiting a nodular appearance (GGNs), compared to 45% (48/106) of benign GGOs (p<0.0001). Conversely, only 5% (1/21) of malignant GGOs exhibited a non-nodular appearance, compared to 55% (58/106) of benign GGOs. There was no significant difference in the mean and standard deviation of attenuation between malignant and benign GGOs.

The mean SUVmax was significantly higher for benign than malignant GGOs (p=0.0017; Figs 5 and 6). The same result was found for mean $SUVmax_{corr\ (normalised\ for\ liver)}$, with even greater statistical significance (p=0.0001). The mean SUVmax for benign GGOs was 1.61, with a range of 0.3–8.8. The mean SUVmax for malignant GGOs was 0.76, with a range of 0.48–1.5 (p=0.0017). An SUVmax cut-off of ≤1.5 yielded a sensitivity for malignancy of 100% and a specificity of 31%. Only 14% (3/21) of the malignant GGOs had an SUVmax >1.

Table 3
Demographics of study cohort.

Characteristic	Benign GGOs (n=106)	Malignant GGOs (n=21)	p-Value
Gender			
Male	59	9	0.34
Female	47	12	
Age (years±SD)	59±16	72±9	0.0002
Smoker (current/former)			
Yes	67	16	0.32
No	39	5	
History of lung cancer			
Yes	30	18	<0.0001
No	76	3	
History of other cancer			
Yes	71	2	<0.0001
No	35	19	

GGOs, ground-glass opacities.

Analysis of the GGN subgroup again revealed the mean SUVmax and $SUVmax_{corr\ (normalised\ for\ liver)}$ to be significantly higher for benign than malignant GGNs (p=0.03 and p=0.0048, respectively). The mean SUVmax for benign GGNs was 1.47 (range 0.3–8.8) and the mean SUVmax for malignant GGNs was 0.73 (range 0.48–1.50). Table 4 summarises the PET/CT imaging findings pertinent to benign and malignant GGOs/GGNs.

Discussion

Radiologists and other healthcare providers often rely upon ^{18}FDG-PET/CT imaging to distinguish malignant from benign pulmonary nodules, guiding clinical management toward or against diagnostic intervention, with high SUVmax numbers widely interpreted as favouring malignancy. More recent studies have shown benign subsolid nodules to demonstrate greater ^{18}F-FDG avidity than malignant subsolid nodules, but did not distinguish part-solid nodules from pure GGNs in their analysis.[19–21] The present study examines and compares the ^{18}F-FDG avidity of benign and

Table 2
Criteria used to determine benignity versus malignancy of the GGOs and number and percentage of GGOs meeting each of these criteria.

Final diagnosis	How diagnosis was made	No. of GGOs (%)
Benign (n=106)	Resolved	79 (75%)
	Decreased in size and attenuation from a prior study over 3 months or longer	2 (2%)
	New (≥1 cm) within 3 months	13 (12%)
	Stable for ≥60 months	4 (4%)
	Imaging features evolved in a manner consistent with interstitial lung disease or radiation fibrosis	8 (8%)
Malignant (n=21)	Increase in size over a >6 month interval	13 (62%)
	Increase in attenuation over a >6 month interval	5 (24%)
	Biopsy/resection	3 (14%)

GGOs, ground-glass opacities.

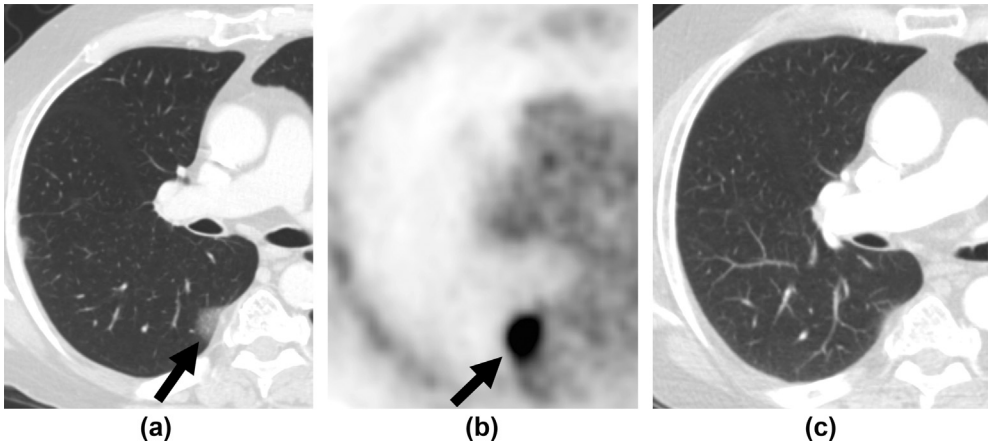

Figure 5 A 51-year-old man with a history of head and neck cancer and (a) an 18 mm mean diameter GGN in the right lower lobe on axial CT (arrow). (b) Corresponding FDG-PET image demonstrates intense FDG uptake (SUVmax = 8.8; arrow). (c) This GGN resolved on follow-up CT 3 months later, in the absence of therapy and was deemed benign.

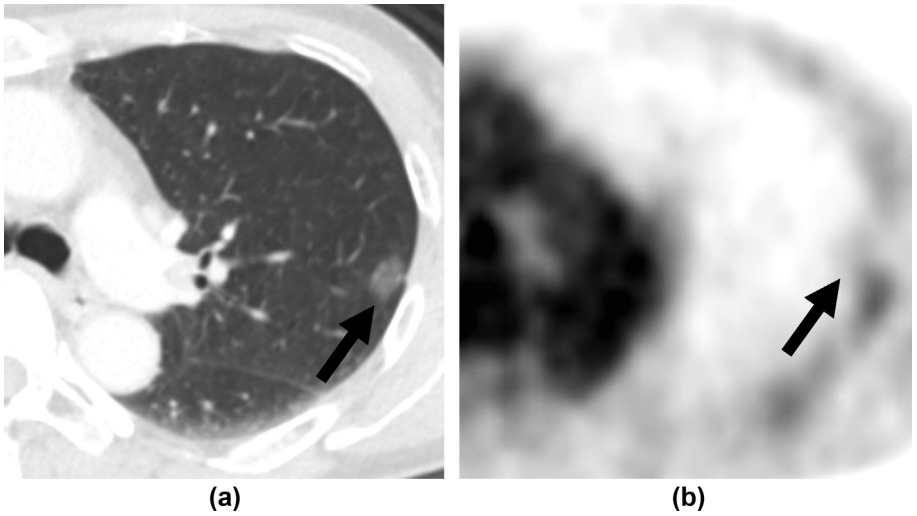

Figure 6 A 64-year-old woman with a history of breast cancer and (a) an 11 mm mean diameter, GGN in the left upper lobe on axial CT (arrow). (b) Corresponding FDG-PET image demonstrates minimal FDG uptake (SUVmax = 0.8; arrow). This GGN was resected and proven malignant. Primary lung adenocarcinoma was confirmed at histopathology.

malignant pure GGOs (nodular and non-nodular) exclusively, using the more clinically practical and widely accepted Fleischner definition, rather than histograms, to classify a pulmonary opacity as ground glass.

In the present study cohort, which included patients with any indication for PET/CT on a single system in the year 2011, the mean SUVmax of GGOs and the GGN subgroup was significantly higher for benign than malignant GGOs/GGNs. In fact, all GGOs and subgroup GGNs with an SUVmax >1.5 were benign. Conversely, no malignant GGO exceeded an SUVmax of 1.5. If the originally cited and later discounted 2.5 threshold for malignancy[8–11] had been used in the present study, all benign GGOs and subgroup GGNs would have been misclassified as malignant.

This paradoxical finding corroborates that of Wu *et al.*, who reported an SUVmax of 1.04±0.43 in their smaller sample size of malignant pure GGNs (n=10)[14] and validates the work of Chun *et al.*;[20] however, the present study had a larger sample size and employed the standard definition of a GGO, used in daily clinical practice, rather than histogram analysis. Histogram analysis risks inclusion of part-solid nodules in a ground-glass cohort, based on reference to the figures and legends of the paper,[23] which provided the methodology for use of histograms in Nomori *et al.*[19] and Chun *et al.*[20]

Reflection on this seeming paradox of benign pure GGOs/GGNs exhibiting greater FDG avidity than their malignant counterparts reveals it not to be a paradox at all. Given the notorious indolence of malignant GGNs, with doubling times of 1.5–3 years,[28,29] it is quite credible that inflammatory ground-glass lesions are typically more metabolically active than their malignant counterparts. Awareness of this finding may prevent misinterpretation of highly ^{18}FDG-avid pure GGOs/GGNs as malignant, which could lead to unnecessary thoracic intervention and its associated risks.

Table 4
Imaging features of pure ground-glass opacities (GGOs), including pure ground-glass nodules (GGN) subgroup, in study cohort on combined 2-[^{18}F]-fluoro-2-deoxy-D-glucose (^{18}FDG) positron-emission tomography/computed tomography (PET/CT).

Characteristic	Benign Total GGOs: n=106; GGN subgroup: n=48	Malignant Total GGOs: n=21 GGN subgroup: n=20	p-Value
Mean size (mm)[a]			
GGO	25.1±15.3	13.6±3.7	<0.0001
GGN subgroup	18.3±7.9	13.7±3.9	0.0112
Lobe			
RUL	37	1	
RML	10	1	
RLL	24	3	
LUL	23	12	
LLL	12	4	0.0088
Morphology			
Nodular (GGN)	48	20	
Non-nodular	58	1	<0.0001
Attenuation value (mean)[a]			
GGO	−548.8±131.5	−542.7±154.3	0.93
GGN subgroup	−528.8±137.2	−539.1±157.4	0.75
SUVmax[a]			
GGO	1.61±1.49	0.76±0.29	0.0017
GGN subgroup	1.47±1.49	0.73±0.26	0.03
$SUVmax_{corr}$ (normalised for liver)[a]			
GGO	0.75±0.64	0.33±0.13	0.0001
GGN subgroup	0.7±0.68	0.33±0.13	0.0048

RUL = right upper lobe, RML = right middle lobe, RLL = right lower lobe, LUL = left upper lobe, LLL = left lower lobe, $SUVmax_{corr}$ = corrected SUVmax, mean ± SD = mean ± one standard deviation, $SUVmax_{corr}$ (normalised for liver)[a].
[a] Mean±SD.

The present study also found that GGOs ≥1 cm in mean diameter, with nodular (GGN), rather than non-nodular, morphology have a high statistical likelihood of malignancy; that malignant GGOs more typically occurred in the upper lobes than benign GGOs; and that a history of lung cancer, and, independently, advanced age conferred a higher likelihood of malignancy to a GGO; however, a history of smoking did not.

The present results further corroborate the value of distinguishing nodular from non-nodular GGOs in terms of predicting benignity and malignancy. Such a distinction has been proven possible by both standard and low-dose chest CT.[30–32]

Limitations

Limitations to this study include its retrospective nature, which was largely countered by randomly sorted, blinded examination of all chest PET/CT examinations performed for any indication (not just those referred for pulmonary nodule evaluation) on a single PET/CT system in the year 2011, after the above-specified exclusions. Use of a single system facilitated a consistent product, including a 1.5 mm thin section series. Second, in most cases, determination of benign or malignant diagnosis required deduction on the basis of GGO/GGN behaviour over time, rather than histopathology. Although the present conclusions would have been more powerful had a greater number of incontestably proven cancers been included, this was not possible because, in clinical practice, most GGNs undergo surveillance, rather than biopsy, until they declare themselves as likely cancers by development of a solid component or an at least part-solid appearance. The recently updated, evidence-based 2017 Fleischner Society guidelines for the management of pulmonary nodules state that both pure GGNs and part-solid nodules of any size which have been stable for 5 years require no further imaging follow-up, inferring the benignity of these nodules. This criterion for benignity was employed in the present study. The present use of rapid development of a ≥1cm mean diameter GGO/GGN over 3 months as a criterion for benignity was based on studies showing a very slow mean volume doubling time (VDT) of malignant GGOs, including a study of adenocarcinomas presenting as GGOs of 813 days[28] and another study showing the VDT of 567±168 days for bronchioloalveolar carcinoma (as it was called at the time of that study) and 384±212 days for adenocarcinoma with bronchioloalveolar carcinoma components.[29] Third, the number of malignant, as opposed to benign, GGNs in the present cohort was relatively small (20 versus 48, respectively). It would not have been appropriate, however, to enhance this number artificially by eliminating randomisation, hand-selecting patients, or including more than one CT examination of a given patient in the year 2011, because it would have risked artificially weighting the data. Despite the small sample size of this cohort, many results achieved statistical significance, substantiating sufficient statistical power. Fourth, data clustering is another possible limitation, because up to five GGOs per patient were included. A statistical method, such as a generalised estimating equation approach, was not used to manage these issues; however, because some patients had a mixture of malignant and benign GGOs. In addition, studies have suggested that multifocal adenocarcinomas behave in an independent manner,[33,34] mitigating this issue. Last, while 100% of the malignant GGNs exhibited an SUVmax ≤1.5 in the present study, validation in another cohort would be needed before employing this SUVmax threshold in any way other than a rough guide in clinical practice. The year 2011 was chosen for this investigation, rather than later years, to assure potential of 5 years of follow-up for every GGO. Earlier years could not be studied because thin 1.5 mm slices were not standard in the diagnostic PET/CT protocol before 2011.

In conclusion, the results of this investigation highlight a potential risk of FDG-PET imaging misinterpretation, which has previously not been fully considered in the context of pure GGOs/GGNs, related to higher metabolic activity of inflammatory lesions and the lower metabolic activity of indolent lung cancer. When employing this concept in clinical practice, it is critical that the Fleischner definition of GGOs be strictly adhered to and supplemented by good clinical judgment. This study suggests that the greater the ^{18}FDG-PET avidity of a pure GGO, or pure GGN more specifically, the more likely it is to be benign. Further validation in a larger study population would be helpful.

Conflicts of interest

None.

References

1. Godoy MC, Naidich DP. Overview and strategic management of subsolid pulmonary nodules. *J Thorac Imag* 2012;**27**:240–8.
2. Chang JM, Lee HJ, Goo JM, *et al*. False positive and false negative FDG-PET scans in various thoracic diseases. *Kor J Radiol* 2006;**7**:57–69.
3. Higashi K, Ueda Y, Seki H, *et al*. Fluorine-18-FDG PET imaging is negative in bronchioloalveolar lung carcinoma. *J Nucl Med* 1998;**39**:1016–20.
4. Kuriyama K, Seto M, Kasugai T, *et al*. Ground-glass opacity on thin-section CT: value in differentiating subtypes of adenocarcinoma of the lung. *AJR Am J Roentgenol* 1999;**173**:465–9.
5. Berger KL, Nicholson SA, Dehdashti F, *et al*. FDG PET evaluation of mucinous neoplasms: correlation of FDG uptake with histopathologic features. *AJR Am J Roentgenol* 2000;**174**:1005–8.
6. Herder GJ, Golding RP, Hoekstra OS, *et al*. The performance of (18)F-fluorodeoxyglucose positron emission tomography in small solitary pulmonary nodules. *Eur J Nucl Med Mol Imag* 2004;**31**:1231–6.
7. Kim TJ, Lee KW, Kim HY, *et al*. Simple pulmonary eosinophilia evaluated by means of FDG PET: the findings of 14 cases. *Kor J Radiol* 2005;**6**:208–13.
8. Patz Jr EF, Lowe VJ, Hoffman JM, *et al*. Focal pulmonary abnormalities: evaluation with F-18 fluorodeoxyglucose PET scanning. *Radiology* 1993;**188**:487–90.
9. Coleman RE. PET in lung cancer. *J Nucl Med* 1999;**40**:814–20.
10. Hashimoto Y, Tsujikawa T, Kondo C, *et al*. Accuracy of PET for diagnosis of solid pulmonary lesions with ^{18}F-FDG uptake below the standardized uptake value of 2.5. *J Nucl Med* 2006;**47**:426–31.
11. Lowe VJ, Fletcher JW, Gobar L, *et al*. Prospective investigation of positron emission tomography in lung nodules. *J Clin Oncol* 1998;**16**:1075–84.
12. Kim BT, Kim Y, Lee KS, *et al*. Localized form of bronchioloalveolar carcinoma: FDG PET findings. *AJR Am J Roentgenol* 1998;**170**:935–9.
13. Yap CS, Schiepers C, Fishbein MC, *et al*. FDG-PET imaging in lung cancer: how sensitive is it for bronchioloalveolar carcinoma? *Eur J Nucl Med Mol Imag* 2002;**29**:1166–73.
14. Wu HB, Wang L, Wang QS, *et al*. Adenocarcinoma with BAC features presented as the nonsolid nodule is prone to be false-negative on ^{18}F-FDG PET/CT. *Biomed Res Int* 2015;**2015**:243681.
15. Gould MK, Maclean CC, Kuschner WG, *et al*. Accuracy of positron emission tomography for diagnosis of pulmonary nodules and mass lesions: a meta-analysis. *JAMA* 2001;**285**:914–24.
16. Kim SK, Allen-Auerbach M, Goldin J, *et al*. Accuracy of PET/CT in characterization of solitary pulmonary lesions. *J Nucl Med* 2007;**48**:214–20.
17. Ruilong Z, Daohai X, Li G, *et al*. Diagnostic value of ^{18}F-FDG-PET/CT for the evaluation of solitary pulmonary nodules: a systematic review and meta-analysis. *Nucl Med Commun* 2017;**38**:67–75.
18. Cronin P, Dwamena BA, Kelly AM, *et al*. Solitary pulmonary nodules: meta-analytic comparison of cross-sectional imaging modalities for diagnosis of malignancy. *Radiology* 2008;**246**:772–82.
19. Nomori H, Watanabe K, Ohtsuka T, *et al*. Evaluation of F-18 fluorodeoxyglucose (FDG) PET scanning for pulmonary nodules less than 3 cm in diameter, with special reference to the CT images. *Lung Cancer* 2004;**45**:19–27.
20. Chun EJ, Lee HJ, Kang WJ, *et al*. Differentiation between malignancy and inflammation in pulmonary ground-glass nodules: the feasibility of integrated (18)F-FDG PET/CT. *Lung Cancer* 2009;**65**:180–6.
21. Tsushima Y, Tateishi U, Uno H, *et al*. Diagnostic performance of PET/CT in differentiation of malignant and benign non-solid solitary pulmonary nodules. *Ann Nucl Med* 2008;**22**:571–7.
22. Hansell DM, Bankier AA, MacMahon H, *et al*. Fleischner Society: glossary of terms for thoracic imaging. *Radiology* 2008;**246**:697–722.
23. Nomori H, Ohtsuka T, Naruke T, *et al*. Histogram analysis of computed tomography numbers of clinical T1 N0 M0 lung adenocarcinoma, with special reference to lymph node metastasis and tumour invasiveness. *J Thorac Cardiovasc Surg* 2003;**126**:1584–9.
24. Collins J, Stern EJ. Ground-glass opacity at CT: the ABCs. *AJR Am J Roentgenol* 1997;**169**:355–67.
25. MacMahon H, Naidich DP, Goo JM, *et al*. Guidelines for management of incidental pulmonary nodules detected on CT images: from the Fleischner Society 2017. *Radiology* 2017;**284**:228–43.
26. Mueller-Mang C, Grosse C, Schmid K, *et al*. What every radiologist should know about idiopathic interstitial pneumonias. *RadioGraphics* 2007;**27**:595–615.
27. Larici AR, del Ciello A, Maggi F, *et al*. Lung abnormalities at multimodality imaging after radiation therapy for non-small cell lung cancer. *RadioGraphics* 2011;**31**:771–89.
28. Hasegawa M, Sone S, Takashima S, *et al*. Growth rate of small lung cancers detected on mass CT screening. *Br J Radiol* 2000;**73**:1252–9.
29. Takashima S, Sone S, Li F, *et al*. Indeterminate solitary pulmonary nodules revealed at population-based CT screening of the lung: using first follow-up diagnostic CT to differentiate benign and malignant lesions. *AJR Am J Roentgenol* 2003;**180**:1255–63.
30. Canellas R, Ackman JB, Digumarthy SR, *et al*. Submillisievert chest dual energy computed tomography: a pilot study. *Br J Radiol* 2018;**91**:20170735.
31. Moyer VA. Force USPSTF. Screening for lung cancer: U.S. Preventive Services Task Force recommendation statement. *Ann Intern Med* 2014;**160**:330–8.
32. Kubo T, Ohno Y, Takenaka D, *et al*. Standard-dose vs. low-dose CT protocols in the evaluation of localized lung lesions: capability for lesion characterization-iLEAD study. *Eur J Radiol Open* 2016;**3**:67–73.
33. Nanki N, Fujita J, Hojo S, *et al*. Evaluation of the clonality of multilobar bronchioloalveolar carcinoma of the lung: case report. *Am J Clin Oncol* 2002;**25**:291–5.
34. Barsky SH, Grossman DA, Ho J, *et al*. The multifocality of bronchioloalveolar lung carcinoma: evidence and implications of a multiclonal origin. *Mod Pathol* 1994;**7**:633–40.